Journal of the Korean Nuclear Society
Volume 17, Number 2, June, 1985

Improved GLR Method to Instrument Failure Detection

Hak Yeoung Jeong and and Soon Heung Chang
Korea Advansed Institute of Science and Technology
(Received November 20, 1984)

측정기기 고장진단에 관한 개선된 GLR방식

정 학 영·장 순 흥
한국과학기술원
(1984. 11. 20 접수)

Abstract

The Generalized Likelihood Ratio (GLR) method performs statistical tests on the innovations sequence of a Kalman-Buchy filter state estimator for system failure detection and its identification. However, the major drawback of the conventional GLR is to hypothesize particular failure type in each case. In this paper, a method to solve this drawback is proposed. The improved GLR method is applied to a PWR pressurizer and gives successful results in detection and identification of any failure. Furthermore, some benefit on the processing time per each cycle of failure detection and its identification can be accompanied.

요 약

GLR (Generalized Likelihood Ratio)방식은 최적상태변수 추정기인 Kalman-Buchy 필터로부터 발생되는 연속 Innovation들에 대해 통계확률적검사를 수행함으로써 시스템 고장 탐지 및 종류를 판별하게 된다. 그러나, 이러한 종전의 GLR방식은 각 경우마다 특별한 고장 형태를 가정해야 하므로, 모든 가능한 고장 형태를 탐지하는 데 많은 어려움이 있다. 이번 논문에서는 이런 난제를 해결할 한 방법을 제시하였다. 그리고, 가압경수형 원자력발전소 일차측 압력을 조절하는 가압기에 적용시켜 본 결과, 어떤 형태의 고장이든 잘 탐지되고 그 종류도 구별할 수 있음을 보여주었으며, 종전방식에 비해 고장 탐지 및 고장 구별에 필요한 컴퓨터처리 시간도 줄일 수가 있었다.

Nomenclature

A	linearized continuous pressurizer model system matrix
a	argumented state
A_p	inches of pressurizer water level per unit water volume (in./ft^3)
B	linearized continuous pressurizer model input matrix
C	linearized pressurized model output matrix
E	expectation operator
f	nonlinear pressurizer model state function
g	nonlinear pressurizer model output function
G	failure signature matrix
GLR	Generalized Likelihood Ratio
h_{cl}	enthalpy of water in primary loop cold leg (Btu/lbm)

h_f pressurizer saturated liquid enthalpy (Btu/lbm)

h_g pressurizer saturated vapor enthalpy (Btu/lbm)

h_p enthalpy of fluid mixture in pressurizer (Btu/lbm)

h_{spray} enthalpy of pressurizer spray flow (Btu/lbm)

h_{surge} enthalpy of pressurizer surge flow (Btu/lbm)

H_a argumented discretized pressurizer model output matrix

H_i *failure hypothesis associated with failure* type i

H_0 no failure hypothesis

i failure type index

I identity matrix

J cost function or units conversion factor (ft^3-psi/Btu)

J_i failure type i information matrix

k discrete current time index

K Kalman filter gain matrix

$\bar{L}$ average pressurizer water level (in.)

L_p pressurizer water level (in.)

LOFT Loss-of-Flow Test

M_p mass of *fluid mixture in pressurizer (lbm)*

M_v mass of vapor in pressurizer (lbm)

M_w mass of water in pressurizer (lbm)

MLE Maximum Likelihood Estimate

MLLR Maximum Log-Likelihood Ratio

N_f number of possible failure types

p Kalman filter estimate error covariance matrix

p finite sampling duration

p_p pressurizer pressure (psia)

Δp_{surge} pressure drop across the pressurizer surge line (psid)

PWR Pressurized Water Reactor

Q Kalman filter process noise covariance matrix

Q_{htr} total pressurizer heating (Btu/s)

R Kalman filter measurement noise covariance matrix

t time (s)

T sample time step (s)

T_p actual pressurizer saturated liquid temperature (°F)

T_{pm} measured pressurizer saturated liquid temperature (°F)

u pressurizer model input vector

$\bar{u}$ valve of u at linearized model operating point

δu perturbation of u from the operating point

v measurement noise vector

v_f *pressurizer saturated liquid specific volume* (ft^3/lbm)

v_g pressurizer saturated vapor specific volume (ft^3/lbm)

v_p specific volume of fluid mixture in pressurizer (ft^3/lbm)

V innovations covariance matrix

V_p total volume of pressurizer (ft^3)

V_{spray} pressurizer spray flow capacity (ft^3/s)

V_w volume of water in perssurizer (ft^3)

w process noise vector

W_{rv} pressurizer total relief valve flow (lbm/s)

W_{spray} pressurizer spray flow (lbm/s)

W_{surge} *pressurizer surge flow (lbm/s)*

x pressurizer model state vector

$\hat{x}$ Kalman filter estimate of x

$\bar{x}$ value of x at linearized model operating point

δx perturbation of x from the operating point

X_p quality of fluid mixture in pressurizer

y pressurizer model output vector

$\bar{y}$ value of y at linearized model operating point

δy perturbation of y from the operating point

γ Kalman filter innovations vector

γ_0 *unfailed system innovations vector*

$\delta(t)$ Kronecker delta function(impulse function)

ε maximum log-likelihood ratio failure detection threshold

θ discrete failure time index.
θ most likely or estimated failure time
Θ discrete pressurizer model input matrix
ν failure magnitude vector
σ estimated value of failure magnitude vector
δ unit step function
τ pressurizer water temperature sensor time constant(s)
Φ discrete pressurizer model state transition matrix
Ω failure perturbation matrix

I. Introduction

In rather a complicated, delicate but large-scale system such as nuclear power plant, it is imperative to monitor the behavior of sensors which continuously check the plant status and also to provide the operator with the stable information for plant parameter identification and compensation. Several instrument failure detection schemes have been studied in the past few years [1-10].

Kalman-Buchy filter is a mathematical algorithm that generates optimal estimate of the plant states using the system dynamics.

One of these instrument failure detection schemes is the GLR technique which performs a statistical tests on the innovations sequence of Kalman-Buchy filter designed for the operating dynamic system and produce a extremely powerful ability of identifying failure type, detecting the failure time, and estimating the magnitude of failure. The innovations can be obtained by subtracting the estimated measurements, which are obtained through Kalman-Buchy filter dynamics from the actual plant measurements.

However, the major difficulty of the conventional GLR approach to failure detection is to hypothesize particular failure types, which may preclude the detection of all possible failures [5]. In coventional GLR method to detect and identify a system failure, specific failure types are hypothesize and their effects on the system dynamics are modeled using failure signature matrices.

Next, it is assumed that a failure of a certain type at a specific time has occurred and the failure magnitude is then estimated.

For each assumed failure, the computed and maximized log-likelihood ratio, as a final step, is compared to a predetermined threshold value to see whether a failure occurred or not.

But, there are actually various types of failure that can happen to appear from the implementation of digital computer to the actual system, plant operation, environmental noises, and the wrong calibration of the instrument, etc.

Unfortunately, it is almost impossible to assume all kinds of failure type in mathematical models, that is, failure signature matrices in advance.

One way to settle down this problem is propossed by using a idea from the concept of "impulse" function in this study [11]. In discrete time domain, the "step" function in continuous time domain can be regarded as sequential collections of a series of impluse train with the same magnitude. Similarily, "ramp" function can be thought of as sequential collections of impulse train with the growing or decreasing magnitude.

Based on these facts, anyfailure type can be represented as a series impluse train so that all that should be done is only to hypothesize the "impluse" failure type. Therefore, this method can be used as a tool of generalization of almost all the possible types of failure with proper failure identification scheme.

In the process of the failure identification, it is possible to identify what kind of failure it is and to determine when the failure occurred based on the information from color CRT(cath-

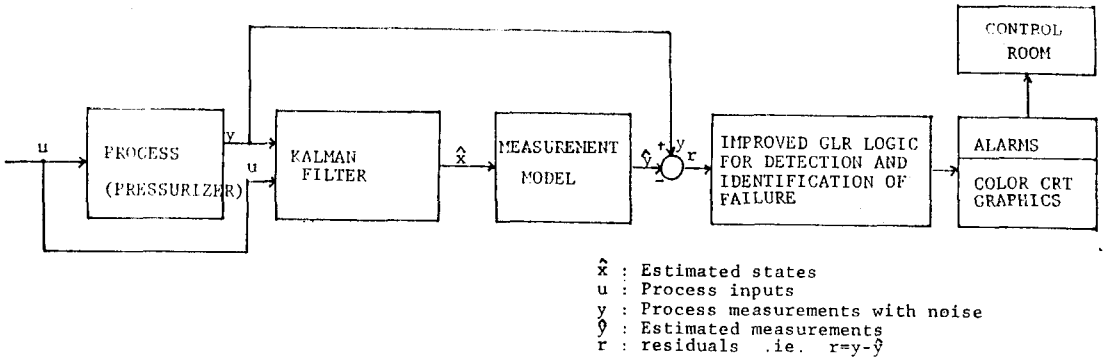

Fig. 1. Kalman Filter and Improved GLR Logic for Detection and Identification of a Failure.

ode ray tube) graphics and alarm system if the color CRT graphics can display at least 20~30 past values of the magnitude of each type of failure.

The overall schematic diagram is shown in Figure 1. The following sections consist of Kalman-Buchy Filter Equations, the method description of the improved GLR techniqne, the application of the improved method to PWR pressurizer, and results and discussion.

II. Kalman-Buchy Filter Equations

Kalman-Buchy filter is simply a mathematical algorithm that generates optimal estimate of the plant state $X(k)$ using the system dynamics and the noise model.

Without using the current measurement $Y(k)$, we already have a prior estimate of the state, $X(k|k-1)$, at the time of the current measurement. Then the problem is to update this estimate based on the current measurement.

The optimal state estimation solution is basically given by the recursive weighted least-square solution.

As a result, the following equations can be formed. The estimate of the current plant state using the current measurement can be given as follows;

$$X(k|k)=X(k|k-1)+K(k)[y(k)-H(k)X(k|k-1)]. \quad (1)$$

The propagation goes ahead in time using the following equation;

$$X(k+1|k)=\phi(k+1,k)X(k|k)+\theta(k)u(k), \quad (2)$$

where $X(k|k-1)$ is state estimation vector at k based on measurements up to time $k-1$, and $K(k)$ is the steady state Kalman-Buchy gain matrix, given in the following from;

$$K(k)=p(k|k-1)H(k)[H(k)P(k|k-1)H(k)^T+R]^{-1}. \quad (3)$$

where $p(k|k-1)$ is the steady-state estimator error covariance matrix which is obtained by solving the algebraic Riccati equation, and calculated from following equations;

The update equation

$$p(k|k)=[I-K(k)]p(k|k-1) \quad (4)$$

and the propagation equation

$$p(k+1|k)=\phi(k+1,k)P(k|k)\phi(k+1,k)^T+Q \quad (5)$$

where R: measurement noise covariance matrix.

Q: process noise covariance matrix.

II-A. Filter Innovations

The filter will generate *a* $r(k)$ vector that is zero-mean and white as follows;

$$r(k)=y(k)-\hat{Y}(k)=y(k)-H(k)\hat{X}(k|k-1). \quad (6)$$

where $r(k)$: innovation (or residual, vector).

Furthermore, for a steady-state Kalman-Buchy filter, the innovation covariance matrix is constant and given by

$$E\{r(k)r(j)^T\}=V(k)\delta(k,j) \tag{7}$$

where

$$V(k)=H(k)p(k\ k-1)H^T(k)+R \tag{8}$$

$$\delta(k,j)=\begin{cases}0, & k\neq j\\ 1, & k=j\end{cases} \tag{9}$$

III. Method Description for Improved GLR

The conventional generalized likelihood ratio (GLR) technique performs statistical tests on the innovations sequence of the Kalman filter state estimator. By using the results of these tests, failures in the sensors of any system are detected and identified. However, this conventional GLR technique involves some difficulties. Some of these are;

(1) A special failure type must be hypothesized in each case in advance, which may preclude the detection of all possible failures because there are actually various types of failure that can happen to appear from the implementation of digital computer to the system, plant operation, environmental noises, and the wrong calibration of instruments, etc.

(3) Much processing time is required for identifying a failure type, which may lead to failure in real-time operation with other purposes (i.e., control, etc).

So that, one way to solve these problems is proposed in this section by using an idea from the concept of "impulse" function. Let us first consider the analysis of a sampled-data system, which is the output of the finite-pulsewidth sampler with an uniform sampling period T and a finite sampling duration p. Fig. 3 illustrates a set of typical input and output signals of the sampler in Fig. 2.

With the notation of Figs. 2 and 3, the output of the finite-pulsewidth sampler is written;

$$r^*_p(t)=r(t)\sum_{k=0}^{\infty}[U_S(t-kT)-U_s(t-kT-p)]. \tag{10}$$

where $U_s(t)$: the unit step function.

$$U_s(t)=\begin{cases}1, & t\geq 0\\ 0, & t<0\end{cases} \tag{11}$$

For $p\ll T$, the narrow-width pulses of Fig. 3 may be approximated by flat-topped pulses. In other words, Eq. (10) can be written

$$r^*_p(t)\cong\sum_{k=0}^{\infty}r(kT)\,[U_s(t-kT)-U_s(t-kT-p)] \tag{12}$$

Multiplying both sides of Eq. (11) by $\frac{1}{p}$ and taking the limit as p approaches zero give;

$$\lim_{p\to 0}\frac{1}{p}r^*_p(t)=\lim_{p\to 0}\sum_{k=0}^{\infty}\frac{1}{p}r(kT)\ [U_s(t-kT)$$

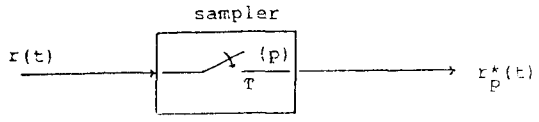

Fig. 2. Block Diagram of a Finite-Pulsewidth Sampler.

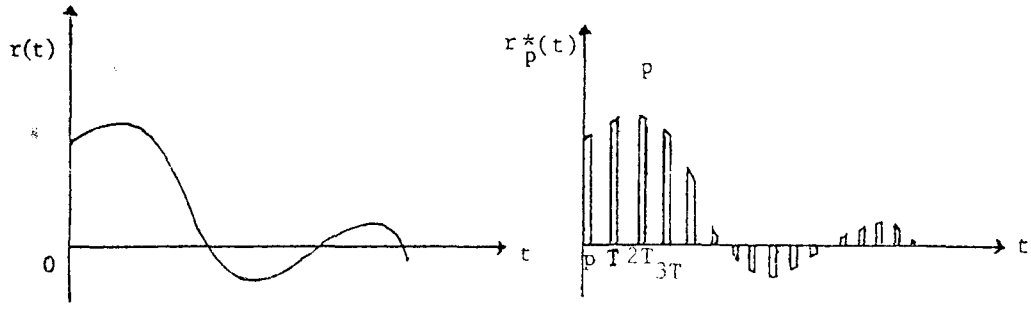

Fig. 3. Input and Output Signals of a Finite-Pulsewidth Sampler.

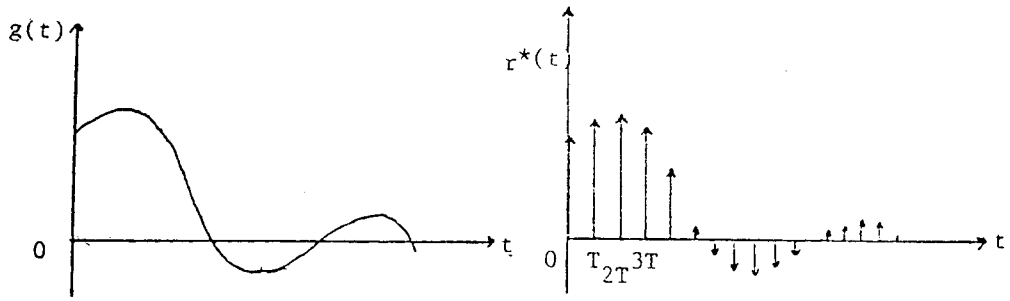

Fig. 4. Input and Output Signals of an Ideal Sampler.

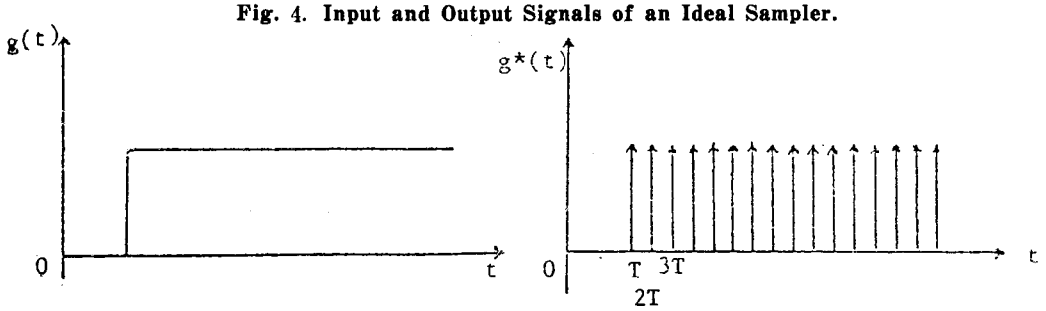

Fig. 5. Input Signal g(t) and Output Signal g*(t) of an Ideal Sampler.

$$-U_s(t-kT-p)] \tag{13}$$

$$=\sum_{k=0}^{\infty} r(kT)\ \delta(t-kT), \tag{14}$$

or

$$\lim_{p\to 0}\frac{1}{p}r_p^*(t)\cong r^*(t). \tag{15}$$

where

$$\delta(t)\triangleq\lim_{p\to 0}\frac{1}{p}[U_s(t)-U_s(t-p)]\text{: impulse function.} \tag{16}$$

The significance of Eq.(15) is that the output of the finite-pulsewidth sampler can be approximated by a train of impulses if the pulsewidth approaches zero in the limit.

If input $r(t)$ in Fig. 3 is passed through the ideal sampler whose output is a train of impulses with the strength of each impulse equal to the magnitude of the input at the corresponding sampling instant, figure 4 illustrates the typical input and output signals of an ideal sampler.

In view of these considerations, the ideal sampler is used to represent the discrete data, $r(kT)$.

Similarly, the step function in continuous time domain also can be expressed as the sequential collections of a series of impulse train as shown in Fig. 5.

Supposing unknown failure type happen to occur, this unknown failure can be treated as impulse at the sampling instant.

Therefore, it is only necessary to hypothesize failure type "impulse" to generalize almost all the possible failure types.

Consider the jump impulse failure in the sensor output and in the state. This failure will appear as additive term in the state and measurement model equations of the form

$$x(k+1)=\phi(k+1,k)x(k)+\theta(k)u(k)+w(k)+\nu\delta(k,j), \tag{17}$$

and $$y(k)=Hx(k)+V(k)+\nu\delta(k,j). \tag{18}$$

where $$\delta(k,j)=\begin{cases}1, & k=j\\ 0, & k\neq j,\end{cases} \tag{19}$$

ν=failure magnitude vector.

This failure takes the from of perturbation in output measurement, $\delta y(k)$.

This effect of a system failure is modeled as follows:

$$\delta y(k)=\Omega_i(k,j)\ \nu_i(k,j), \tag{20}$$

where $\Omega_i(k,j)$=the failure perturbation matrix for impulse failure type at time j,

and $\Omega_i(k,j)$ is $\Omega_i(k,j)=\begin{cases}0, & k<j\\ I, & k=j\\ 0, & k>j.\end{cases}$ (21)

where I=a identify matrix.

Since the Kalman filter equations are also linear, the resulting perturbation in the plant measurement will propagate through the equations yielding a new innovations equation of the form

$$r(k)=G_i(k,j)\nu_i(k,j)+r_0(k),\quad k\geqq j. \tag{22}$$

where

$r(k)$ =innovations of the failed system at time k,

j =time of system failure,

$\nu_i(k,j)$=impulse failure magnitude vector,

$r_0(k)$ =innovations sequence of the unfailed system,

$G_i(k,j)$=failure signature matrix for impulse failure.

To evaluate $G_i(k,j)$, Eq. (20) is substituted into the Kalman filter equations and the resulting effect on the innovations is calculated.

This results in the recursive equations:

$$G_i(k,j)=\Omega_i(k,j)-H\Phi F_i(k-1,j), \tag{23}$$

$$F_i(k,j)=KG_i(k,j)+\Phi F_i(k-1,j), \tag{24}$$

$$G_i(k,j)=F_i(k,j)=0,\quad k<j. \tag{25}$$

where K=the Kalman gain matrix.

At each time k, one must determine whether impulse failure has occurred or not.

This requires the selection of one of the hypotehses: No failure hypothesis H_0 is

$$\sqrt{k}=r_0(k). \tag{26}$$

A impulse failure hypothesis H_i is

$$r(k)=G_i(k,j)\nu_i(k,j)+r_0(k). \tag{27}$$

We can then perform the GLR test to decide if a impulse failure has occurred. Essentially, we compute the maximum likelihood estimate (MLE), ν(k) of the failure magnitude based on $r(1),\cdots r(k)$ and $G_i(k,j)$.

These values are then used in computing the log-likelihood ratio $l(k)$ for H_i versus H_0, given the observed innovations $r(1),\cdots,r(k)$.

After some mathematical manipulations, we can have

$$\nu_i(k,j)=J_i^{-1}(k,j)d_i(k,j), \tag{28}$$

$$J_i(k,j)=G_i^T(k,j)\,V^{-1}(k)G_i(k,j), \tag{29}$$

$$d_i(k,j)=G_i^T(k,j)\,V^{-1}(k)r(k), \tag{30}$$

$$l_i(k,j)=d_i^T(k,j)\nu_i(k,j). \tag{31}$$

Our decision rule is

$$l_i[k,j]\underset{H_0}{\overset{H_i}{\lesseqgtr}}\varepsilon. \tag{32}$$

where ε is a threshold value chosen to provide a reasonable trade-off between false and missed alarms.

Accepting Ho indicates that no failure exists. If H_i is accepted, however, the assumption is that "impulse" failure has occurred. Following this detection, failure identification is made when $j=k$, namely, the instant that the failure occurred with the display of the 20~30 past values of the magnitude of the faiure on the color CRT graphics.

IV. Application to PWR Pressurizer

The nonlinear LOFT pressurizer model developed by J.L. Tylee is admitted without great modification in this study. The required discretization step for the use of failure detection is presented here. In the model introduced in this section, steam and water in the pressurizer are

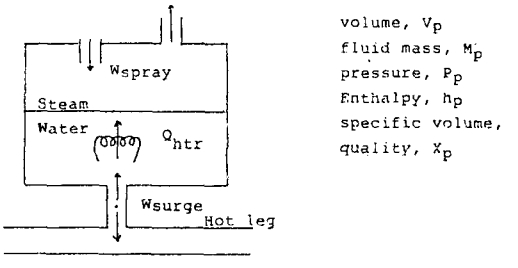

Fig. 6. Pressurizer Model.

assumed to be in a homogeneous saturated mixture. The typical PWR pressurizer is shown schematically in Fig. 6.

Applying mass and energy balances to this mixture results in the following two equations;

$$\frac{dM_p}{dt} = W_{surge} + W_{spray}. \tag{33}$$

$$\frac{d(M_p h_p)}{dt} = \frac{V_p}{J}\frac{dP_p}{dt} + Q_{htr} + W_{spray}h_f + W_{spray}h_{spray} - W_{rv}h_g. \tag{34}$$

The desired state variables for the pessurizer model are P_p, pressure, and X_p, mixture quality. Equations for these variables are obtained by noting the following equations;

$$V_p = V_p/M_p = v_f + X_p(v_g - v_f), \tag{35}$$

$$h_p = h_f + X_p(h_g - h_f). \tag{36}$$

where

t : the continuous time variable.

J : a units conversion factor

h_f : the saturated water enthalpy.

h_g : the saturated steam enthalpy.

h_{spray} : the known spray flow enthalpy.

v_f, v_g : the specific volumes of saturated water and stream, respectively.

By substituting Eqs. 35 and 36 into Eqs. 33 and 34, one can solve simultaneously for $\frac{dP_p}{dt}$ and $\frac{dX_p}{dt}$. This rather lengthy manipulation yields;

$$\frac{dP_p}{dt} = \frac{-v_p}{V_p\Omega}\{v_p\frac{\partial h_p}{\partial X_p}(W_{surge} + W_{spray} - W_{rv}) + \frac{\partial v_p}{\partial X_p}[Q_{htr} + W_{surge}(h_f - h_p) + W_{spray}(h_{spray} - h_p) - W_{rv}(h_g - h_p)]\}, \tag{37}$$

$$\frac{dX_p}{dt} = \{\frac{v_p}{V_p\Omega}\{v_p(W_{surge} + W_{spray} - W_{rv})\left[\frac{\partial h_p}{\partial P_p} - \frac{v_p}{J}\right] + \frac{\partial v_p}{\partial P_p}[Q_{htr} + W_{surge}(h_f - h_p) + W_{spray}(h_{spray} - h_p) - W_{rv}(h_g - h_p)]\}]. \tag{38}$$

where

$$\Omega = \frac{\partial v_p}{\partial P_p}\frac{\partial h_p}{\partial X_p} - \frac{\partial h_p}{\partial P_p}\left[\frac{\partial h_p}{\partial P_p} - \frac{v_p}{J}\right]. \tag{39}$$

An additional state of interest is the measured temperature of the saturated fluid mixture T_{pm}. Assuming first-order dynamics for the temperature sensor, this measurement can be characterized by the following relation;

$$\frac{dT_{pm}}{dt} = \frac{T_p - T_{pm}}{\tau_p}. \tag{40}$$

where τ_p : time constant.

The surge flow is computed as follows;

$$W_{surge} = \begin{cases} K_s(\Delta P_{surge})^{1/2}, \Delta P_{surge} > 0 \\ -K_s(\Delta P_{surge})^{1/2}, \Delta P_{surge} < 0. \end{cases} \tag{41}$$

where K_s : constant which is determined emperically.

The following pressurizer water level is described by;

$$L_p = A_p(1 - x_p)\frac{V_p}{v_p}v_f. \tag{42}$$

where A_p : conversion constant water volume to water level.

Finally, the nonlinear model is summarized as follow;

$$\dot{x} = f(x, u), \tag{43}$$

$$y = g(x). \tag{44}$$

where $x, u,$ and, y be represented in the following vector forms

$$x = [x_p P_p T_{pm}]^T, \tag{45}$$

$$u = [W_{surge} Q_{htr} W_{spray} W_{rv}]^T, \tag{46}$$

$$y = [L_p P_p T_{pm}]^T. \tag{47}$$

By expanding Eqs. 43 and 44 in Taylor series about a nominal operation point $(\bar{x}, \bar{u})$ (ignoring terms higher than the first order), the linearized form of pressurizer can be obtained. In the following equations, the linearization will provide $A, B,$ and C matrix so that the model can be written in linear, constant coefficient state variable form;

$$\delta\dot{x}(t) = A\delta x(t) + B\delta u(t) \tag{48}$$

and

$$y(t) = c\delta x(t). \tag{49}$$

where

$$\delta x(t) = x(t) - \bar{x}, \tag{50}$$

$$\delta u(t) = u(t) - \bar{u}, \tag{51}$$

$$\delta y(t) = y(t) - \bar{y}. \tag{52}$$

Generally, an IFD (Instrument Failure Detection) scheme will employ a digital computer to make the state estimation and failure detection.

For this reason, the continuous time model Eqs. 48 and 49 must be discretized in the following form;

$$\delta x(k+1)=\Phi(k+1,k)\delta x(k)+\Theta(k+1,k)\delta u(k)+w(k) \quad (53)$$

and

$$\delta y(k)=H(k)\delta x(k)+v(k). \quad (54)$$

where

$$\Phi(k+1,k)=\exp A)\Delta t). \quad (55)$$

$$\Delta t=t_{k+1}-t_k. \quad (56)$$

$$\Theta(k+1,k)=\int_{t_k}^{t_k+1}\Phi(t_{k+1},\tau)B(\tau)d\tau. \quad (57)$$

Finally, Esq. 53 and 54 are the forms required by Kalman-Buchy filter, the improved GLR to failure detection and identification and control.

Note that the matrices Φ, Θ, and H are shift-invariant for the fixed operating point $(\bar{x}, \bar{u})$. (Refer to Appendix A)

V. Results and Discussion

The computer simulation has been made on LOFT pressurizer in case of a system failure to test the improved GLR method. The program is programmed in FORTRAN and runs in real time.

Several sets of simulation are stored on magnatic disks and compared with actual LOFT data in Fig. 7, 8. For the verification of the pressurizer model have been performed in Fig. 8 for the system transient where the surge flow is treated as the system transient.

One cycle of failure detection and its identification requires 170 msec of IBM-370 processing time. This is desirable since preliminary simulation studies showed that sampling the plant measurement every second provides excellent failure detection and its identification. The remaining time (830 msec) in each cycle of the process allows for further expansion in pressurizer modelling and some considerations on Kalman-Buchy filter gain.

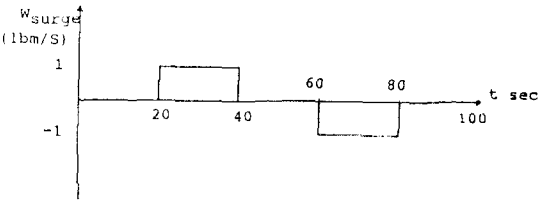

Fig. 7. The Simulated Disturbance for Verification of Pressurizer Model.

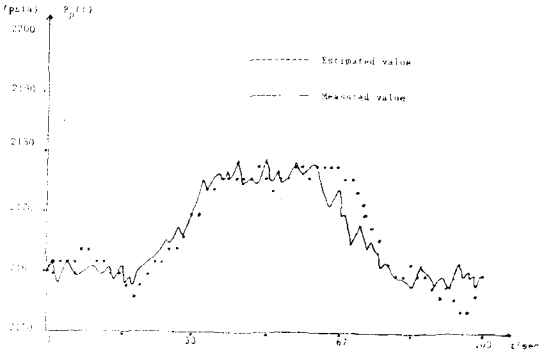

Fig. 8. Pressurizer Pressure Resopnse for System Transient in Fig. 7.

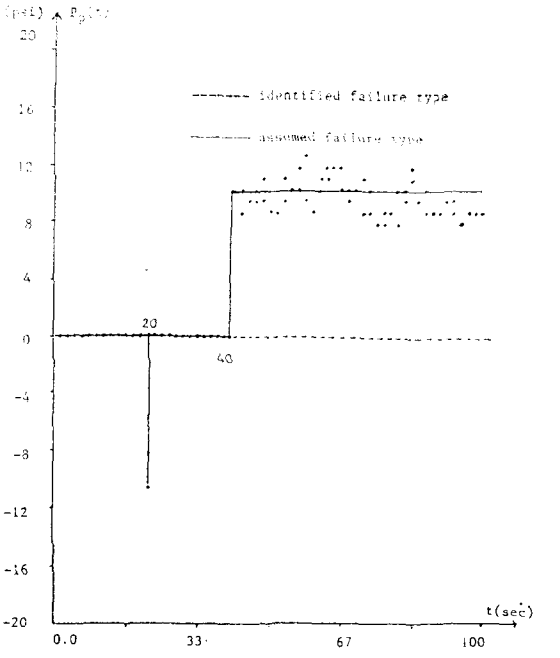

Fig. 9. Jump at 20 sec and Step at 40 sec in Pressure State.

Table 1. Comparison of Processing Time on IBM 370 Computer.

Method	Improved GLR	Conventional GLR
Processing Time	180 msec	290msec

In this study, the threshold value ε was chosen 20 based on the sensitivity analysis at a norminal condition. Fig. 9 through 18 shows the assumed failure types and the corresopnding identified failured types.

Note that the solid lines in Fig. 9 through 18 are the assumed failure types while the dotted lines in Fig. 9 through 18 are the corresponding identified failure types. Table 1 shows the comparison of the processing time per cycle of the improved GLR method with that of the conventional GLR method for failure detection and its identification. As shown in Fig. 9 through 18, Table 2, and Table 3, the improved method for online any failure detection and its identification gives successful results.

Note that each magnitude of identified failure for failure type "step" may have some range

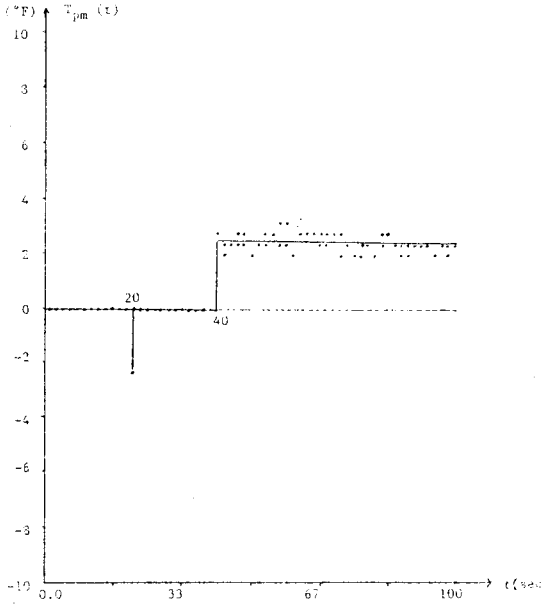

Fig. 10. Jump at 20sec and Step at 40sec in Temperature State.

because failure type "step" is based on the collection of a series of failure type "jump". Each time the failure is detected and identified, there can be a little overestimation or underestimation over failure magnitude due to estimation error

Table 2. Results of "Jump" Failure Type Case.

Assumed failure	Detection time	Identified Failure	MLLR
−0.015 jump in in quality state	20 sec	−0.0155	0.1956 E+4
−10 jump in pressure state	20 sec	−10.5 psi	0.3960 E+2
−2.5°F jump in temperature state	20 sec	−2.53° F	0.6250 E+2
−0.5 inch jump in level sensor	20 sec	−0.417 in.	0.3722 E+2
10 psi jump in pressure sensor	20 sec	9.55 psi	0.3266 E+2
−2.5°F jump in temperature sensor	20 sec	−2.53° F	0.6250 E+2

where MLLR means maximum log-likelihood ratio.

Table 3. Results of "Step" Failure Type Case.

Assumed Failure	Detection time	Identified failure	MLLR
0.015 step in quality state	40 sec	0.0157	0.1831 E+4
10 psi step in pressure state	40 sec	10.5 psi	0.4167 E+2
2.5°F step in temperature state	40 sec	2.62° F	0.6536 E+2
0.5 inch step in level sensor	40 sec	0.515 in	0.5695 E+2
−10 psi step in pressure sensor	40 sec	−9.46 psi	0.3410 E+2
2.5°F step in temperature sensor	40 sec	2.13° F	0.6536 E+2

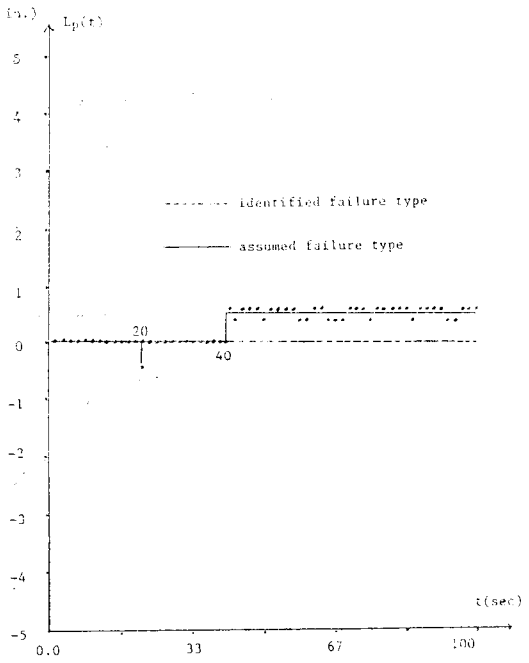

Fig. 11. Jump at 20 sec and Step at 40 sec in Level Sensor.

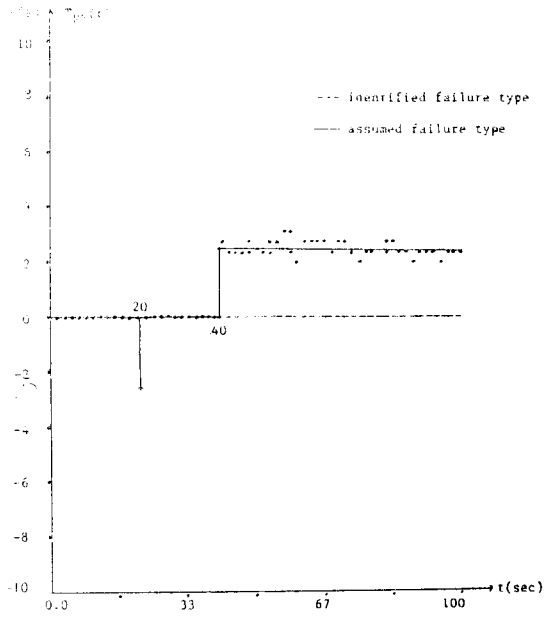

Fig. 13. Jump at 20 sec and Step at 40 sec in Temperature Sensor.

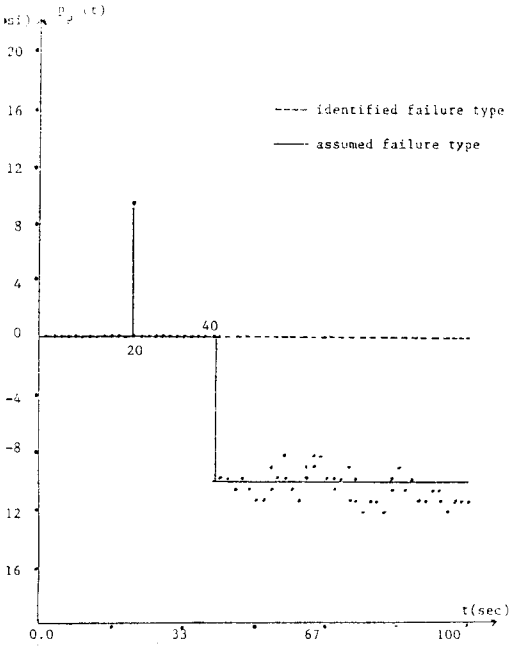

Fig. 12. Jump at 20 sec and Step at 40 sec in Pressure Sensor.

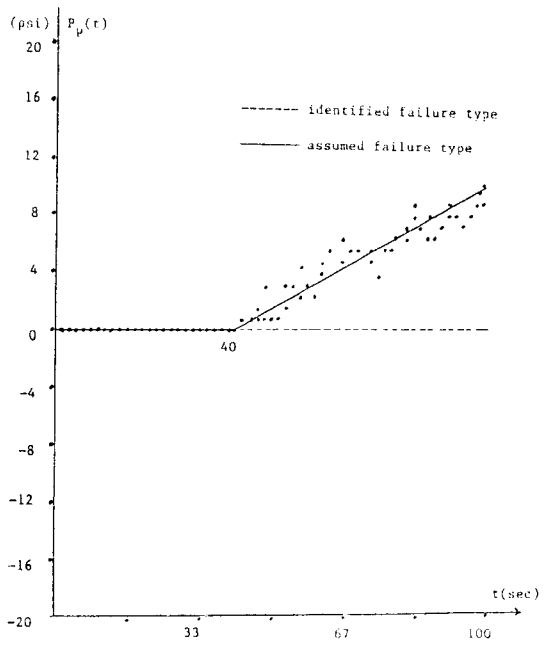

Fig. 14. Ramp at 40sec in Pressure State.

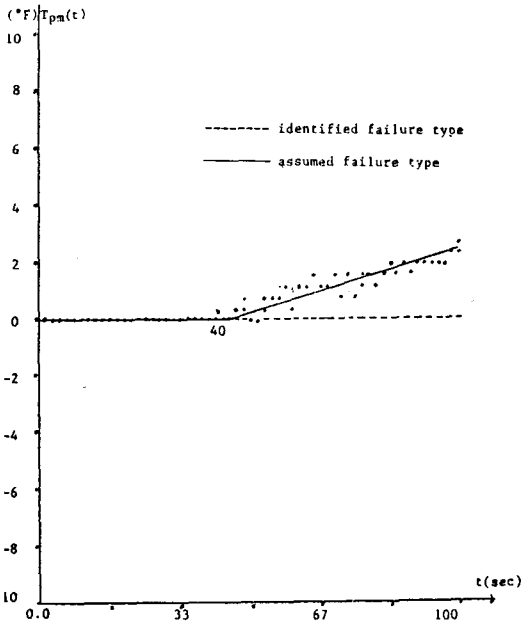

Fig. 15. Ramp at 40 sec in Temperature State.

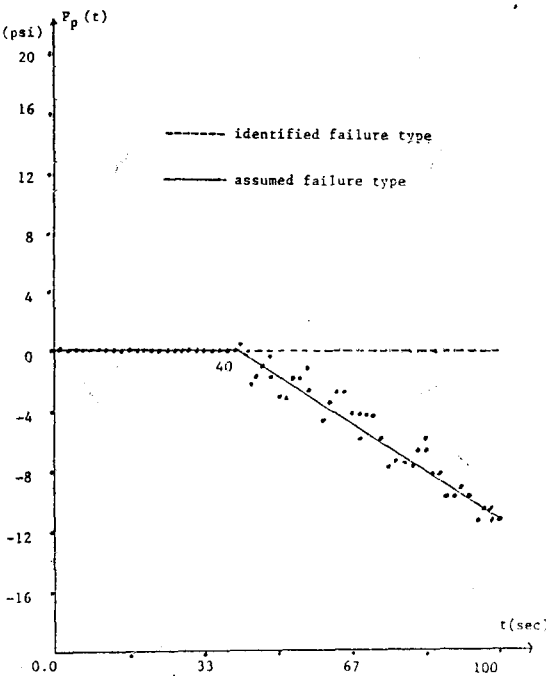

Fig. 17. Ramp at 40sec in Pressure Sensor.

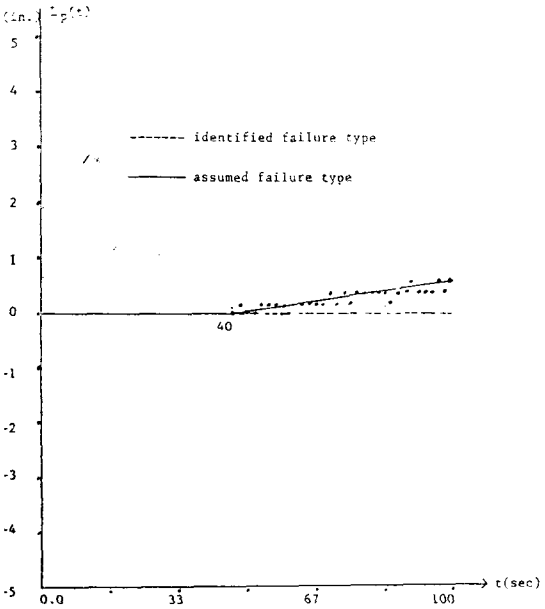

Fig. 16. Ramp at 40sec in Level Sensor.

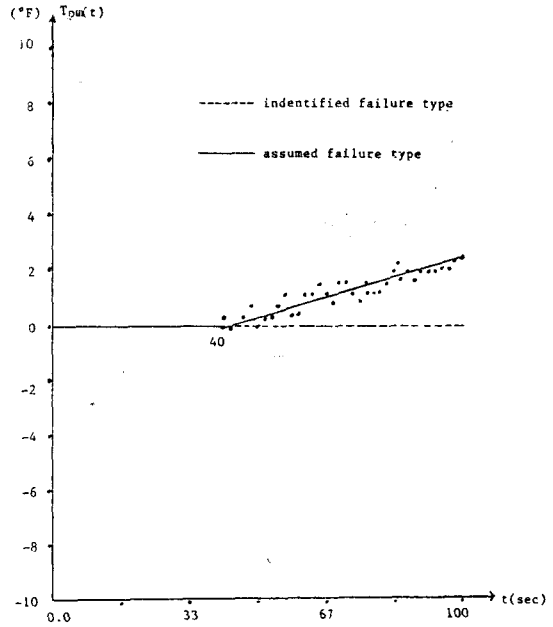

Fig. 18. Ramp at 40sec in Temperature Sensor.

and noise. Therefore, the magnitude of each failure type and maximum log-likelihood ratio (MLLR) were averaged over some identification period in case of "step" type as indicated in Table 3.

VI. Conclusion

In this paper, improved GLR method to detect and identify a failure is developed and is applied to PWR pressurizer. Several capabilities of the improved GLR failure monitor for type of failure have been described and evaluated.

Summarizing some points to consider as follows;

1. It is developed to generalize any kind of failure type by using only "impulse" function concept instead of modelling each failure case by case as does in the conventional GLR method.
2. The improved method is applied to the PWR pressurizer and could perform the tasks of the detection and identification of any failure very successfully.
3. The improved method also have some benefit on processing time compared to the conventional GLR method.
4. This improved GLR method would improve safety and availability by using on-line digital computer to provide information about plant status for the operator via color CRT graphics and alarm system.

References

1. Alans. Willsky, Harold L. Jones, "A Generalized Likelihood Ratio Approach to Detection and Estimation of Jump in Linear System," IEEE Trans. Automat. Contr. Feb., 1976.
2. R.N. Clark, "The Dedicated Observer Approach to Instrument Failure Detection," in Proc. 18th IEEE Conf. Decision Confr. Fort Lauderdale, FL, Dec., 1979.
3. J.L. Tylee, "Real-time Instrument Failure Detection in the LOFT Pressurizer using Functional Redundancy," EG & G Idaho, Inc., Rep. EGG-EE-5518, July, 1982.
4. R.N. Clark and B. Campbell, "Instrument Fault Detection in a Pressurized Water Reactor Perssurizer," Nucl. Technol. Vol. 56, Jan., 1982.
5. J.L. Tylee, "A Generalized Likelihood Ratio Approach to Detecting and Identifying Failures in Pressurizer Instrumentation," Nucl. Technol., Vol. 56, Mar., 1982.
6. J.L. Tylee, "Instrument Failure Detection and Accommodation," EGG-LOFT-5925, Oct., 1982.
7. J.Y. Tylee, "On-Line Failure Detection in Nuclear Power Plant Instrument, "IEEE Tran. Automat. Contr. Vol. Ac-28, No. 3, Mar., 1983.
8. A. Gelb, Ed., Applied Optimal Estimation, Cambridge, MA: M.I.T. Press, 1974.
9. A.P. Sage and J.L. Melsa, Estimation Theory with Applications to Communications and Control, Huntington, NY: Krieger, 1979.
10. Gene F. Franklin and J. David Powell, Digital Control of Dynamic Systems, 1980.
11. Benjamin C. Kue, Automatic Control Systems, the third Edition, 1975.

Appendix A

(Failure Decision System Specifications)

1. Pressurizer model operating point:

$$x=[x_p p_p T_{pm}]^T=\begin{bmatrix}0.0059\\2260.0\\647.4\end{bmatrix}\begin{matrix}(-)\\(\text{psia})\\(^\circ\text{F})\end{matrix}$$

$$u=[Q_{htr}\ W_{\text{spray}}\ W_{ro}]^T=\begin{bmatrix}0.0\\0.0\\0.0\end{bmatrix}\begin{matrix}(\text{Btu/s})\\(\text{lbm/s})\\(\text{lbm/s})\end{matrix}$$

d : disturbance

$d=\theta' W_{\text{surge}}$; $\theta'=[-2.927\times10^{-4}\ \ 0.818\ \ 1.336\times10^{-3}]^T$

$$y=[L_p P_p T_{pm}]^T=\begin{bmatrix}41.90\\2159.20\\647.60\end{bmatrix}\begin{matrix}(\text{in.})\\(\text{psia})\\(^\circ\text{F})\end{matrix}$$

2. Linear, continuous pressurizer model system matrices:

$$\dot{x}(t)=Ax(t)+Bu(t)$$

$$y(t)=Cx(t)$$

$$A=\begin{bmatrix}0.0 & 0.0 & 0.0\\0.0 & 0.0 & 0.0\\0.0 & 0.00332 & -0.05\end{bmatrix}$$

$$B=\begin{bmatrix} -2.927\times10^{-4} & 4.291\times10^{-7} & -3.582\times10^{-4} & 1.065\times10^{-4} \\ 0.818 & 1.008\times10^{-2} & -0.7221 & -5.194 \\ 0.0 & 0.0 & 0.0 & 0.0 \end{bmatrix}$$

$$C=\begin{bmatrix} -194.3 & 0.01507 & 0.0 \\ 0.0 & 1.0 & 0.0 \\ 0.0 & 0.0 & 1.0 \end{bmatrix}$$

3. A Matrix Eignevalues, λ_i, and Eigenvector Matrix Z:

$$\lambda_1=\begin{bmatrix} \lambda_1 \\ \lambda_2 \\ \lambda_3 \end{bmatrix}=\begin{bmatrix} 0.0 \\ -0.05 \\ 0.0 \end{bmatrix}, \qquad Z=\begin{bmatrix} 1.0 & 0.0 & 0.0 \\ 0.0 & 0.0 & 1.0 \\ 0.0 & 1.0 & 0.06641 \end{bmatrix}$$

4. Discrete Pressurizer Model State Transient Matrix, and Input Matrix(calcaulted using a sample time step of T=1 sec)

$$\phi=\begin{bmatrix} 1.0 & 0.0 & 0.0 \\ 0.0 & 1.0 & 0.0 \\ 0.0 & 0.003238 & 0.9512 \end{bmatrix}$$

$$\theta=\begin{bmatrix} 4.291\times10^{-7} & -3.582\times10^{-4} & 1.065\times10^{-4} \\ 1.008\times10^{-2} & -0.7221 & -5.194 \\ 1.647\times10^{-5} & -1.179\times10^{-3} & -8.481\times10^{-3} \end{bmatrix}$$

5. Initial Estimate Error Covariance Matrix Prior to Updating:

$$P(0|-1)=\begin{bmatrix} 7.526\times10^{-5} & 0.0 & 0.0 \\ 0.0 & 8.410 & 0.0 \\ 0.0 & 0.0 & 0.0625 \end{bmatrix}$$

6. Preocess Noise Covariance Matrix

$$Q=\begin{bmatrix} 2.300\times10^{-8} & 0.0 & 0.0 \\ 0.0 & 1.150 & 0.0 \\ 0.0 & 0.0 & 0.02 \end{bmatrix}$$

7. Measurement Noise Covariance Matrix

$$R=\begin{bmatrix} 0.0025 & 0.0 & 0.0 \\ 0.0 & 1.0 & 0.0 \\ 0.0 & 0.0 & 0.0625 \end{bmatrix}$$

8. Compurted Steady State Kalman Gain Km, and Innovation Covariance Matrices

$$K=\begin{bmatrix} -0.0222\times10^{-2} & 0.2694\times10^{-4} & 0.9237\times10^{-6} \\ 0.1684\times10^{1} & 0.6268 & 0.8865\times10^{-2} \\ -0.1147\times10^{-2} & 0.5540\times10^{-3} & 0.4080 \end{bmatrix}$$

$$V=\begin{bmatrix} 0.4772\times10^{-2} & 0.2154\times10^{-1} & 0.1091\times10^{-4} \\ 0.2154\times10^{-1} & 0.2777\times10^{1} & 0.2557\times10^{-2} \\ 0.1091\times10^{-4} & 0.2557\times10^{-2} & 0.1056 \end{bmatrix}$$

Appendix B

(Pressurizer Model Parameters)

1. Pressurizer volume : V_p=34.75 ft^3
2. Pressurizer level conversion constant : A_p=2.02 in./ft^3

3. Spray flow rate : $V_{spray}=0.0446 ft^3/s$(if on)
4. Back up heater capacity : $Q_{bup}=11.37$ Btu/s
5. Cycling heater capacity : $Q_{cyc}=34.12$ Btu/s
6. Power-operated relief valve capacity : $W_{por}=2.0$ lbm/s
   Safety relief valve capacity : $W_{saf}=12.6$lbm/s

(Pressure diagram)